# Supplementary Materials: Robust Inclusion Complex of Topotecan Comprised within a Rhodamine-Labeled β-Cyclodextrin: Competing Protonand Energy Transfer Processes

**Maria Rosaria di Nunzio and Abderrazzak Douhal**

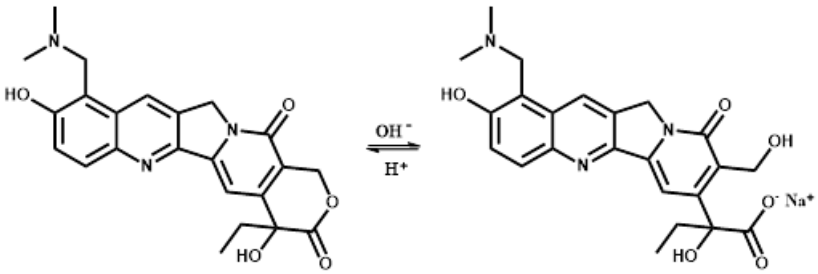


**Scheme S1.** Illustration of the ground-state equilibrium between the lactone and carboxylate forms of TPT in a water solution.

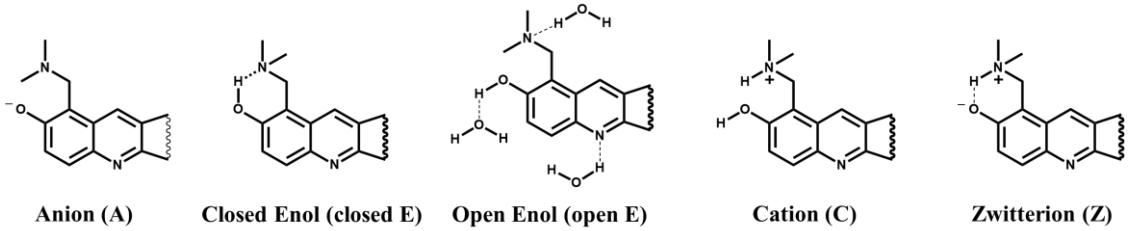


**Scheme S2.** Illustration of the TPT species in water at pH 6.24: anion (A), enol (closed and open E), cation (C), and zwitterion (Z) species. For simplicity, only the quinoline moieties of the structures are shown.

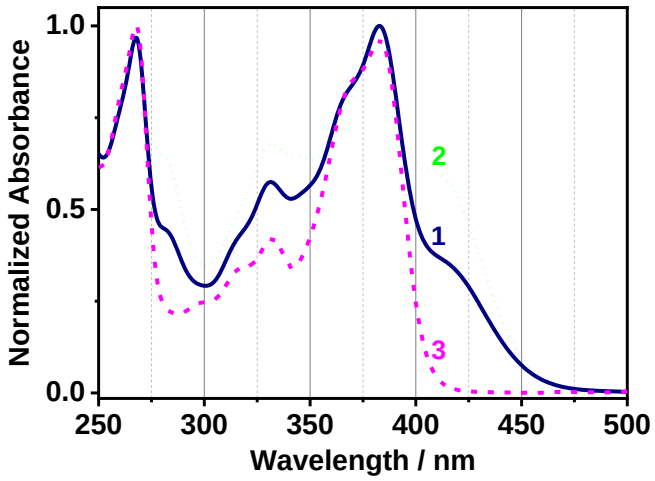


**Figure S1.** Normalized (to the maximum of intensity) absorption spectra of TPT:RB-RM-βCD (1, solid line), TPT:DM-βCD (2, dotted line), and TPT:TM-βCD (3, dashed line) in water at pH ~6.2 (1) or in phosphate-buffered saline (PBS) solutions at pH = 7.23 (2,3).

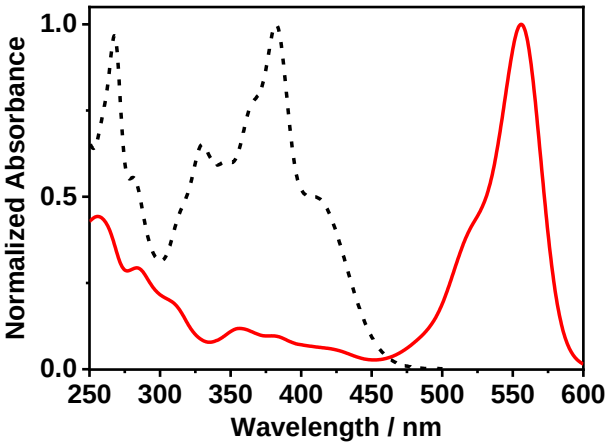


**Figure S2.** Normalized (to the maximum of intensity, i.e., 382 and 556 nm for TPT and RB-RM-βCD, respectively) absorption spectra of TPT (black dashed line) and RB-RM-βCD (red solid line) in water solutions (pH ~6.2).

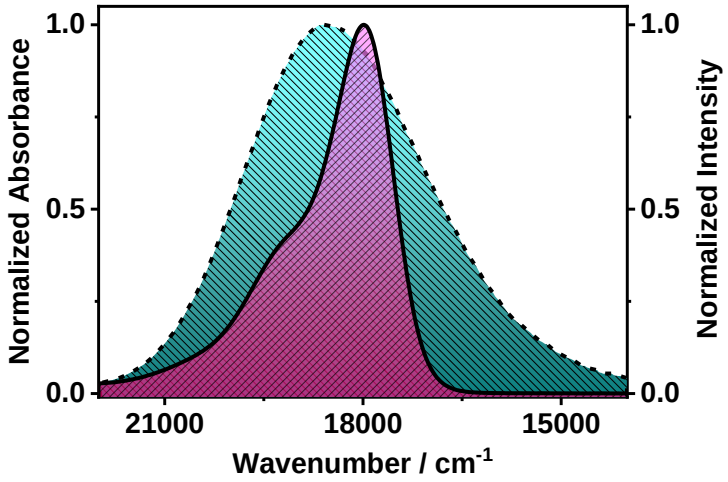


**Figure S3.** Normalized (to the maximum of intensity) absorption (solid line) and emission (dashed line) spectra of TPT and RB-RM-βCD, respectively, in water solutions (pH ~6.2).

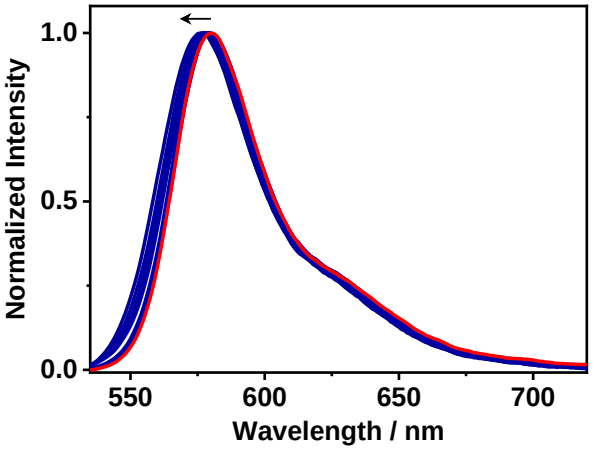

**Figure S4.** Normalized emission spectra of RB 2.9 μM in water solutions (pH ~6.2) without (red line) and after (blue lines) the addition of DM-βCD in different concentrations (from 0.2 to 20 mM). The blue-shifted spectra are corrected for the dilution effect.

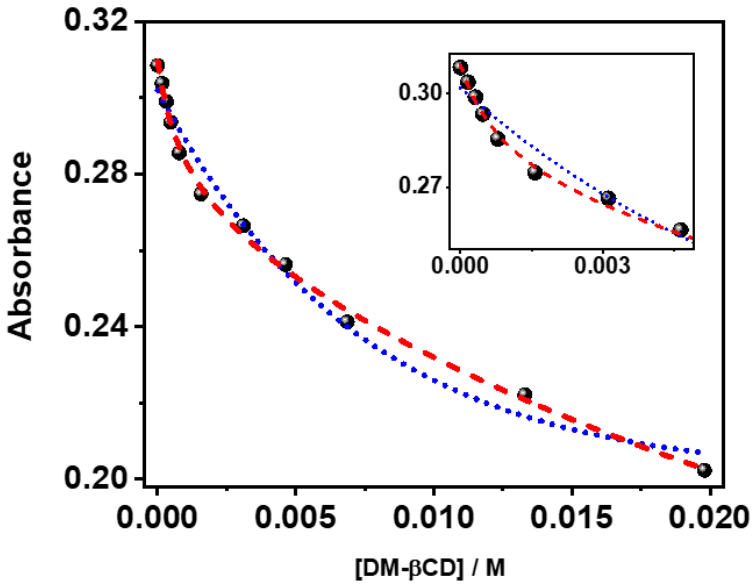


**Figure S5.** Absorbance variation of RB in water at pH ~6.2 with DM-βCD concentration observed at 554 nm. The red dashed line is from the best fit assuming the formation of 1:1 and 1:2 complexes, while the blue dotted one is from the best fit only assuming the formation of the 1:1 complex. Insert: the zoom of Figure S4 at low DM-βCD concentrations.

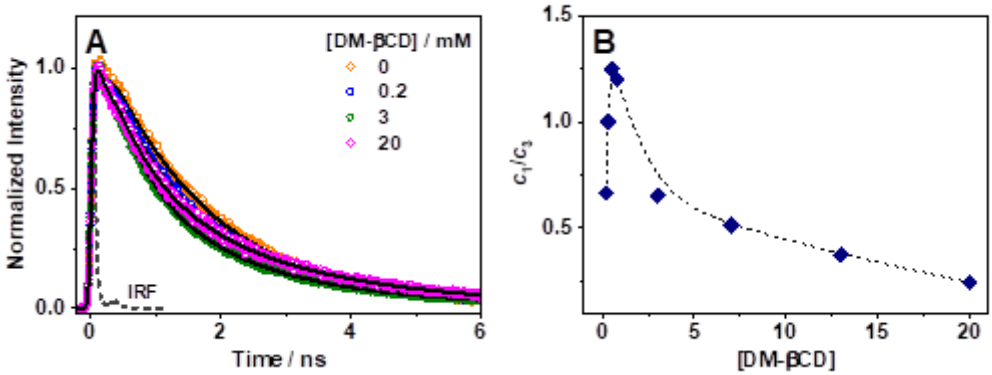


**Figure S6.** (A) Normalized (to the maximum of intensity) ps-emission decays of RB 2.9 μM in water solutions (pH ~6.2) without and after the addition of DM-βCD at different concentrations (0.2, 3, and 20 mM). The excitation and observation wavelengths were 371 and 630 nm, respectively. The solid lines are from the best fit of the experimental data. IRF is the instrumental response function. (B) Dependence of the $c_1$-to-$c_3$ ratio ($c_1/c_3$) with DM-βCD concentration, where $c_1$ and $c_3$ are the contributions of $\tau_1$ and $\tau_3$ components in the emission decays at 630 nm. The dashed line in (B) only serves to guide the eyes.

**Table S1.** Time constants ($\tau_i$), normalized (to 100) pre-exponential factors ($a_i$), and contributions ($c_i$) obtained from the multi-exponential fit of the emission decays of RB 2.9 μM in water solutions (pH ~6.2) without and after the addition of increasing amounts (from 0.2 to 20 mM) of DM-βCD. The excitation was at 371 nm and the observation wavelengths are indicated in the table.

| [DM-βCD] /mM | $\lambda_{obs}$ /nm | $\tau_1$/ps ± 50 | $a_1$ /% | $c_1$ /% | $\tau_2$/ns ± 0.20 | $a_2$ /% | $c_2$ /% | $\tau_3$/ns ± 0.30 | $a_3$ /% | $c_3$ /% |
|---|---|---|---|---|---|---|---|---|---|---|
| 0 | 560 | | | | 1.67 | 100 | 100 | | | |

| | | | | | | | | | | | |
|---|---|---|---|---|---|---|---|---|---|---|---|
| | 580 | | | | | 100 | 100 | | | | |
| | 630 | | | | | 100 | 100 | | | | |
| | 560 | | 20 | 7 | | 76 | 84 | | 4 | 9 | |
| 0.2 | 580 | 560 | 16 | 6 | 1.67 | 80 | 85 | 3.50 | 4 | 9 | |
| | 630 | | 19 | 7 | | 77 | 85 | | 4 | 8 | |
| | 560 | | 27 | 11 | | 70 | 82 | | 3 | 7 | |
| 0.3 | 580 | 590 | 21 | 8 | 1.67 | 76 | 84 | 3.60 | 3 | 8 | |
| | 630 | | 25 | 10 | | 72 | 82 | | 3 | 8 | |
| | 560 | | 31 | 13 | | 67 | 80 | | 2 | 7 | |
| 0.5 | 580 | 600 | 24 | 10 | 1.67 | 73 | 82 | 3.90 | 3 | 8 | |
| | 630 | | 27 | 11 | | 70 | 81 | | 3 | 8 | |
| | 560 | | 35 | 15 | | 62 | 76 | | 3 | 9 | |
| 0.8 | 580 | 590 | 28 | 12 | 1.67 | 68 | 78 | 3.80 | 4 | 10 | |
| | 630 | | 32 | 13 | | 64 | 77 | | 4 | 10 | |
| | 560 | | 46 | 20 | | 43 | 52 | | 11 | 28 | |
| 3 | 580 | 580 | 42 | 17 | 1.67 | 47 | 57 | 3.40 | 11 | 26 | |
| | 630 | | 46 | 20 | | 45 | 56 | | 9 | 24 | |
| | 560 | | 45 | 18 | | 39 | 45 | | 16 | 37 | |
| 7 | 580 | 590 | 42 | 17 | 1.67 | 44 | 50 | 3.40 | 14 | 33 | |
| | 630 | | 47 | 20 | | 41 | 50 | | 12 | 30 | |
| | 560 | | 41 | 15 | | 37 | 38 | | 22 | 47 | |
| 13 | 580 | 580 | 40 | 15 | 1.67 | 42 | 45 | 3.30 | 18 | 40 | |
| | 630 | | 45 | 18 | | 39 | 45 | | 16 | 37 | |
| | 560 | | 35 | 11 | | 34 | 31 | | 31 | 58 | |
| 20 | 580 | 580 | 36 | 12 | 1.67 | 39 | 39 | 3.30 | 25 | 49 | |
| | 630 | | 40 | 15 | | 38 | 40 | | 22 | 45 | |

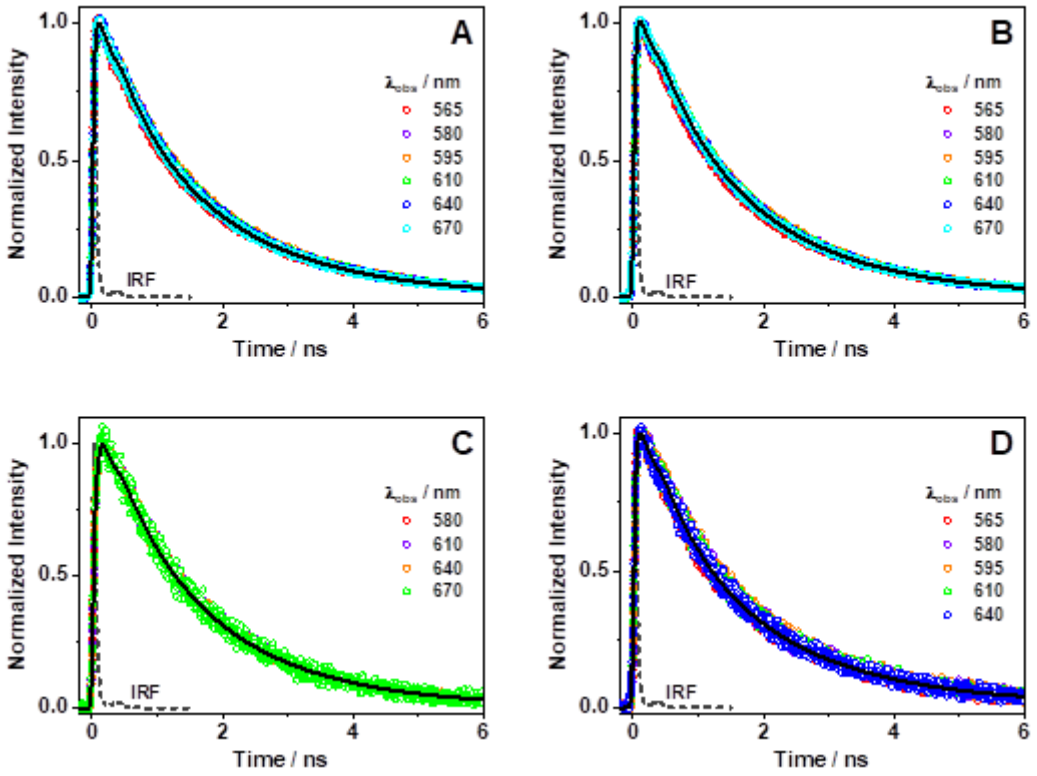


**Figure S7.** Normalized (to the maximum of intensity) ps-emission decays of RB-RM-βCD in PBS solutions (pH = 7.3) at different concentrations: (A) $1.1 \times 10^{-4}$ M, (B) $1.1 \times 10^{-5}$ M, (C) $1.1 \times 10^{-6}$ M, and (D) $1.1 \times 10^{-7}$ M. The excitation wavelength is at 371 nm, while the observation ranges are indicated in the inset. The solid lines are from the best fit of the experimental data. IRF is the instrumental response function.

**Table S2.** Time constants ($\tau_i$), normalized (to 100) pre-exponential factors ($a_i$), and contributions ($c_i$) obtained from the multi-exponential fit of the emission decays of RB-RM-βCD in PBS solutions (pH = 7.3) at four different concentrations of RB-RM-βCD upon excitation at 371 nm and observation as indicated in the table.

| [RB-RM-βCD] /$10^{-7}$ M | $\lambda_{obs}$ /nm | $\tau_1$/ps ± 50 | $a_1$ /% | $c_1$ /% | $\tau_2$/ns ± 0.2 | $a_2$ /% | $c_2$ /% | $\tau_3$/ns ± 0.3 | $a_3$ /% | $c_3$ /% |
|---|---|---|---|---|---|---|---|---|---|---|
| 1.1 | 565 | 580 | 15 | 10 | 1.6 | 79 | 78 | 3.4 | 6 | 12 |
| | 580 | | 17 | 7 | | 78 | 82 | | 5 | 11 |
| | 595 | | 17 | 7 | | 78 | 82 | | 5 | 11 |
| | 610 | | 20 | 9 | | 75 | 80 | | 5 | 11 |
| | 640 | | 22 | 10 | | 73 | 79 | | 5 | 11 |
| 11 | 580 | 580 | 16 | 6 | 1.6 | 79 | 83 | 3.4 | 5 | 11 |
| | 610 | | 18 | 7 | | 77 | 82 | | 5 | 11 |
| | 640 | | 18 | 7 | | 77 | 82 | | 5 | 11 |
| | 670 | | 20 | 8 | | 75 | 80 | | 5 | 12 |
| 110 | 565 | 590 | 26 | 11 | 1.6 | 68 | 77 | 3.3 | 6 | 12 |
| | 580 | | 19 | 8 | | 76 | 82 | | 5 | 10 |
| | 595 | | 18 | 7 | | 77 | 82 | | 5 | 11 |
| | 610 | | 21 | 8 | | 74 | 81 | | 5 | 11 |
| | 640 | | 21 | 8 | | 74 | 82 | | 5 | 10 |
| | 670 | | 22 | 9 | | 73 | 81 | | 5 | 10 |
| 1100 | 565 | 590 | 29 | 10 | 1.7 | 66 | 78 | 3.5 | 5 | 12 |
| | 580 | | 24 | 8 | | 71 | 81 | | 5 | 11 |
| | 595 | | 23 | 8 | | 72 | 81 | | 5 | 11 |
| | 610 | | 25 | 8 | | 71 | 81 | | 4 | 11 |
| | 640 | | 26 | 9 | | 70 | 81 | | 4 | 10 |
| | 670 | | 27 | 10 | | 69 | 80 | | 4 | 10 |

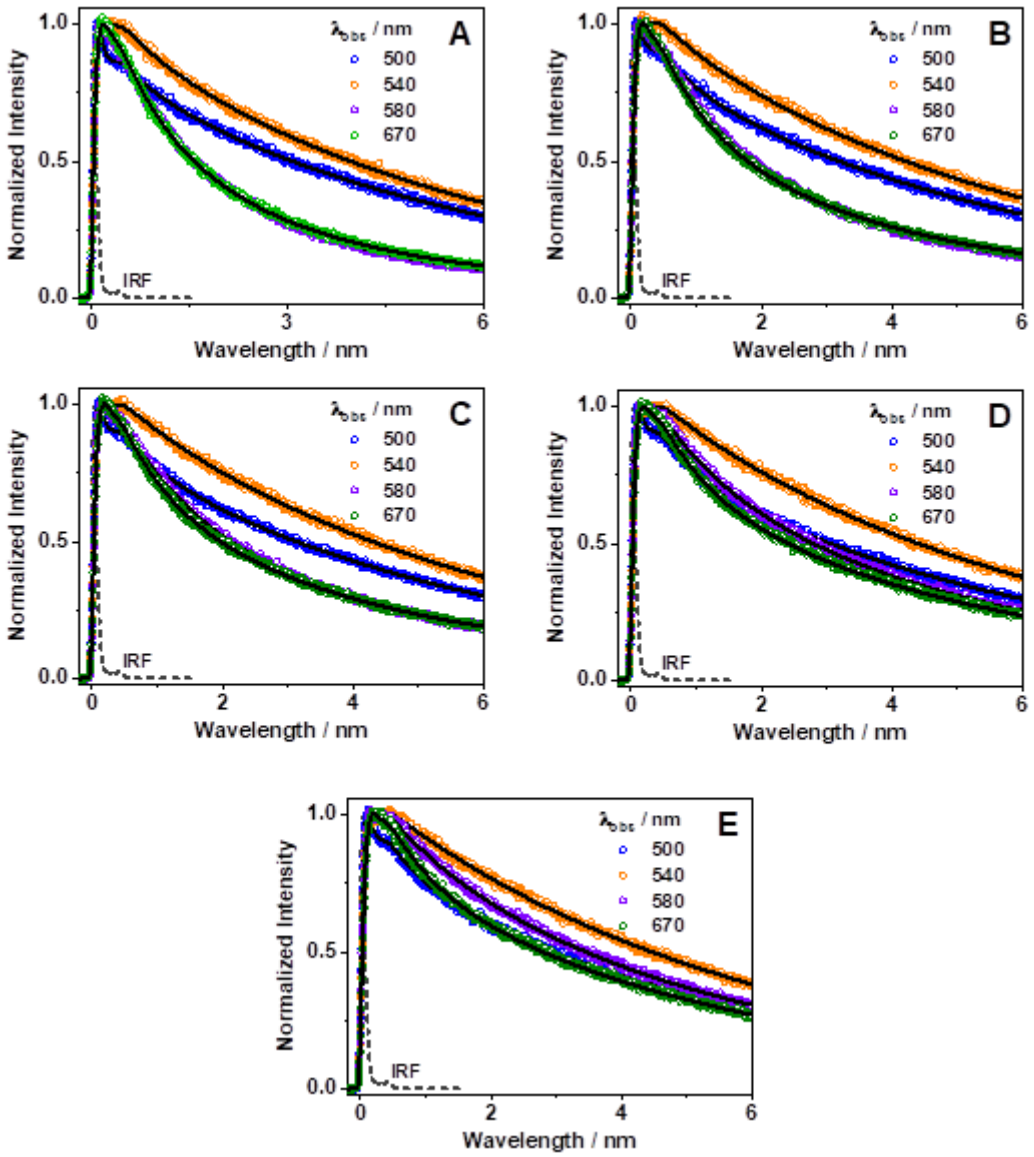


**Figure S8.** Normalized (to the maximum of intensity) ps-emission decays of TPT:RB-RM-βCD in water solutions (pH ~6.2) at five different [guest]/[host] ratios (guest = TPT; host = RB-RM-βCD): (A) 0.38, (B) 0.76, (C) 1.14, (D) 2.27, and (E) 4.16. The excitation wavelength was at 371 nm, while the observation wavelengths are indicated in the inset. The solid lines are from the best fit of the experimental data. IRF is the instrumental response function.

**Table S3.** Time constants ($\tau_i$), normalized (to 100) pre-exponential factors ($a_i$), and contributions ($c_i$) obtained from the multi-exponential fit of the emission decays of TPT:RB-RM-βCD in water solutions (pH ~6.2) at five different [guest]/[host] ratios upon excitation at 371 nm and observation as indicated in the table. The negative signs for $a_1$ and $c_1$ indicate a rising component in the emission signal.

| $\lambda_{obs}$ = 500 nm | | | | | | | | | | | | |
|---|---|---|---|---|---|---|---|---|---|---|---|---|
| $\frac{[guest]}{[host]}$ | $\tau_1$/ps ± 15 | $a_1$ /% | $c_1$ /% | $\tau_2$/ps ± 50 | $a_2$ /% | $c_2$ /% | $\tau_3$/ns ± 0.2 | $a_3$ /% | $c_3$ /% | $\tau_4$/ns ± 0.3 | $a_4$ /% | $c_4$ /% |
| 0.38 | 39 | 52 | 1 | 590 | 8 | 2 | - | - | - | 5.7 | 40 | 97 |
| 0.76 | 39 | 44 | 1 | 590 | 11 | 2 | - | - | - | 5.7 | 45 | 97 |
| 1.14 | 40 | 43 | 1 | 590 | 11 | 2 | - | - | - | 5.6 | 46 | 97 |
| 2.27 | 40 | 40 | 1 | 580 | 13 | 3 | - | - | - | 5.6 | 47 | 96 |
| 4.16 | 40 | 39 | 1 | 580 | 15 | 3 | - | - | - | 5.6 | 46 | 96 |
| $\lambda_{obs}$ = 540 nm | | | | | | | | | | | | |
| $\frac{[guest]}{[host]}$ | $\tau_1$/ps ± 15 | $a_1$ /% | $c_1$ /% | $\tau_2$/ps ± 50 | $a_2$ /% | $c_2$ /% | $\tau_3$/ns ± 0.2 | $a_3$ /% | $c_3$ /% | $\tau_4$/ns ± 0.3 | $a_4$ /% | $c_4$ /% |
| 0.38 | 39 | -100 | -100 | 590 | 9 | 1 | 1.7 | 6 | 2 | 5.7 | 85 | 97 |
| 0.76 | 39 | -100 | -100 | 590 | 6 | 1 | 1.7 | 4 | 1 | 5.7 | 90 | 98 |
| 1.14 | 40 | -100 | -100 | 590 | 6 | 1 | 1.7 | < 1 | < 1 | 5.6 | 94 | 99 |
| 2.27 | 40 | -100 | -100 | 580 | 4 | 1 | 1.7 | < 1 | < 1 | 5.6 | 96 | 99 |
| 4.16 | 40 | -100 | -100 | 580 | 2 | < 1 | 1.7 | < 1 | < 1 | 5.6 | 98 | 100 |
| $\lambda_{obs}$ = 580 nm | | | | | | | | | | | | |
| $\frac{[guest]}{[host]}$ | $\tau_1$/ps ± 15 | $a_1$ /% | $c_1$ /% | $\tau_2$/ps ± 50 | $a_2$ /% | $c_2$ /% | $\tau_3$/ns ± 0.2 | $a_3$ /% | $c_3$ /% | $\tau_4$/ns ± 0.3 | $a_4$ /% | $c_4$ /% |
| 0.38 | 39 | -100 | -100 | 590 | 13 | 4 | 1.7 | 55 | 47 | 5.7 | 32 | 49 |
| 0.76 | 39 | -100 | -100 | 590 | 13 | 3 | 1.7 | 53 | 32 | 5.7 | 34 | 65 |
| 1.14 | 40 | -100 | -100 | 590 | 11 | 2 | 1.7 | 44 | 25 | 5.6 | 45 | 73 |
| 2.27 | 40 | -100 | -100 | 580 | 9 | 1 | 1.7 | 32 | 14 | 5.6 | 59 | 85 |
| 4.16 | 40 | -100 | -100 | 580 | 4 | 1 | 1.7 | 21 | 7 | 5.6 | 75 | 92 |
| $\lambda_{obs}$ = 670 nm | | | | | | | | | | | | |
| $\frac{[guest]}{[host]}$ | $\tau_1$/ps ± 15 | $a_1$ /% | $c_1$ /% | $\tau_2$/ps ± 50 | $a_2$ /% | $c_2$ /% | $\tau_3$/ns ± 0.2 | $a_3$ /% | $c_3$ /% | $\tau_4$/ns ± 0.3 | $a_4$ /% | $c_4$ /% |
| 0.38 | 39 | -100 | -100 | 590 | 25 | 6 | 1.7 | 53 | 38 | 5.7 | 22 | 56 |
| 0.76 | 39 | -100 | -100 | 590 | 26 | 6 | 1.7 | 40 | 24 | 5.7 | 34 | 70 |
| 1.14 | 40 | -100 | -100 | 590 | 27 | 5 | 1.7 | 32 | 18 | 5.6 | 41 | 77 |
| 2.27 | 40 | -100 | -100 | 580 | 26 | 4 | 1.7 | 20 | 10 | 5.6 | 54 | 86 |
| 4.16 | 40 | -100 | -100 | 580 | 25 | 4 | 1.7 | 13 | 5 | 5.6 | 62 | 91 |

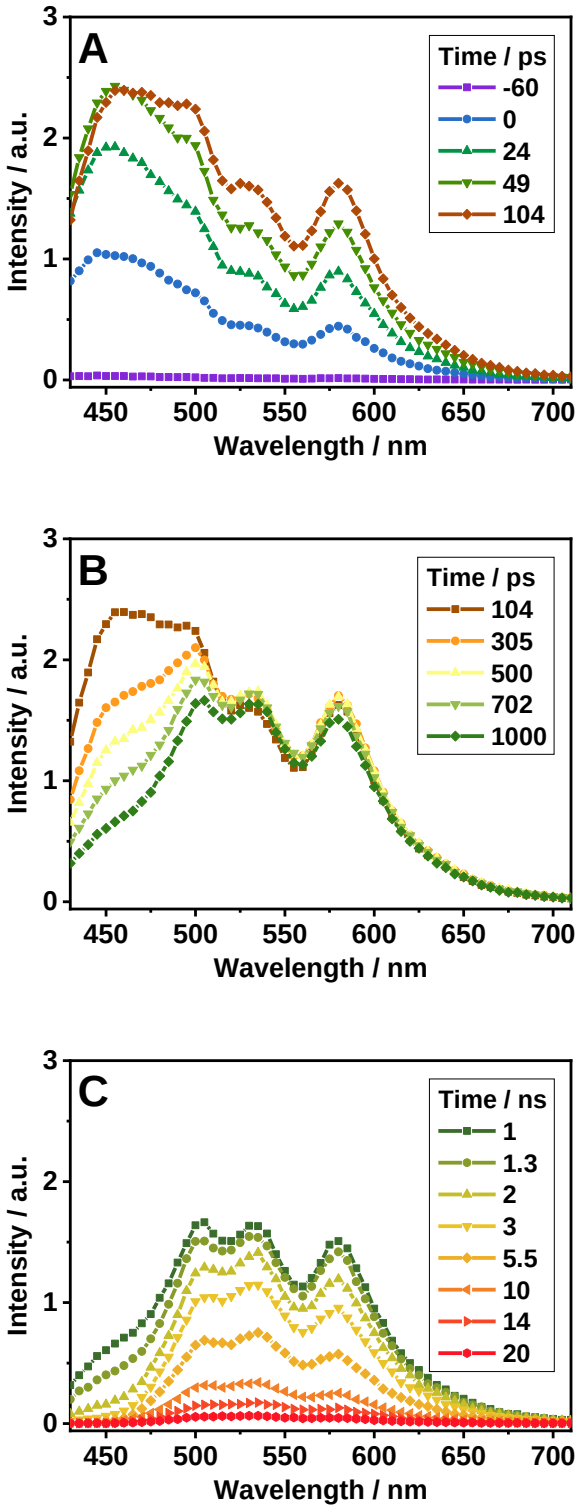


**Figure S9.** TRES of TPT:RB-RM-βCD in a water solution (pH ~6.2) upon ~~the~~ excitation at 371 nm and with a [TPT]/[RB-RM-βCD] value of ~4. The insets indicate the gating times of the TRES. (A): from – 60 to 104 ps, (B): from 104 to 1000 ps and (C): from 1 to 20 ns.

**Table S4.** Observed and corrected ($E_{Obs(c)}$) efficiencies for the ET process involving TPT (5.60 μM) and RB at different concentrations of RB-RM-βCD. f is the molar fraction of the 1:1 complex between TPT and RB-RM-βCD having an equilibrium constant $K_{eq} = 3.7 \times 10^4$ $M^{-1}$ at 20 °C, and $E_{Obs(c)} = E_{Obs}/f$.

| [RB-RM-βCD] / μM | f | $E_{Obs(c)}$ (%) |
|---|---|---|
| 43 | 0.59 | 39 |
| 35 | 0.54 | 41 |
| 25 | 0.45 | 43 |
| 19 | 0.38 | 41 |
| 14.5 | 0.32 | 40 |
| 10.1 | 0.24 | 42 |
| 7.5 | 0.19 | 41 |
| 3.5 | 0.098 | 35 |

**Table S5.** Rotational relaxation times (φ) and molecular volumes ($V_{exp}$) of RB, RB-RM-βCD, and TPT:RB-RM-βCD in PBS solutions at pH 7.41 exciting at 510 and observing at 580 nm. The molecular systems were modeled as ellipsoid, non-hydrated rotors under both stick- and slip-boundary conditions using the Stokes–Einstein–Debye hydrodynamic theory. The calculated parameters are: $\tau_{stick}$, $\tau_{slip}$ (rotational times), and $V_{theor}$ (molecular volume).

| System | A = C / Å | B / Å | Type of ellipsoid | $V_{theor}$[a] / Å$^3$ | f[b] | $\tau_{stick}$ ($\tau_{slip}$) / ps | φ / ps | $V_{exp}$[c] / Å$^3$ |
|---|---|---|---|---|---|---|---|---|
| RB | 9.8 | 14.8 | Prolate | 744 | 1.2 | 221 (23.4 ) | 172 | 728 |
| RB-RM-βCD | 17 | 25 | Prolate | 3783 | 1.2 | 1100 (117) | 219, 859 | 3473[d] |
| TPT:RB-RM-βCD | 17 | 34 | Prolate | 5145 | 1.5 | 1910 (460) | 219, 1280 | 5176[d] |

[a]$V_{theor} = (4\pi a^2 b)/3$, where a = c and b hold for the semi-minor and the semi-major axes of the prolate ellipsoid, respectively. [b]The parameter f is a factor which takes into account the shape of the solute (f = 1 for a sphere, > 1 for non-spherical molecules). [c]$V_{exp} = (\varphi k_B T)/(\eta f C)$, where φ is the experimental rotational time, $k_B$ is the Boltzmann constant ($1.38 \times 10^{-16}$ erg/K), T is the temperature (293 K), η is the viscosity of the medium ($9.55 \times 10^{-3}$ and $11 \times 10^{-3}$ Poise for buffer and buffer in presence of CD, respectively), and C is a factor which is equal to 1 for stick-boundary conditions. [d]Calculated taking into account the longer φ.

**Benesi–Hildebrand (BH) Model**

*BH Model from Absorption Data*

When the cyclodextrin (CD) forms a 1:1 complex with the substrate (S), the binding constant ($K_{eq}$) can be expressed as:

$$K_{eq} = \frac{[S:CD]}{[CD]\cdot[S]} = \frac{X_i}{(C_{CD} - C_S X_i)(1 - X_i)} \quad (S1)$$

where [S:CD], [CD], and [S] are the equilibrium concentrations of the complex, free CD, and free S, respectively. $C_{CD}$ and $C_S$ are the concentrations of CD and S, while $X_i$ = [S:CD]/$C_S$. Assuming that the molar extinction coefficients of the free and caged S at a certain wavelength are $\varepsilon_0$ and $\varepsilon_\infty$, respectively (herein, the absorption of CD is usually equal to 0). Thus, when $C_{CD} = 0$, the absorption of the solution is $A_0 = \varepsilon_0 l C_S$, in which l is the length of the cell. If the analytical concentration of CD is $C_{CD}^i$, the apparent absorption of the solution is $A_i = \varepsilon_0 l C_S(1-X_i) + \varepsilon_\infty l C_S X_i$. If $C_S$ is constant, then $A_i = A_0 + \Delta A X_i$, where $\Delta A = (\varepsilon_\infty - \varepsilon_0) l C_S$. If $C_{CD}^i >> C_S$, the following equation can be obtained:

$$\frac{1}{K_{eq}} = \frac{(C_{CD}^i - C_S X_i)(1 - X_i)}{X_i} = C_{CD}^i \frac{(1 - X_i)}{X_i} = C_{CD}^i \frac{\Delta A}{(\Delta A_i - 1)} \quad (S2)$$

where $\Delta A_i = A_i - A_0 = \Delta A X_i$. Rearrangement of (2) gives:

$$\frac{1}{\Delta A_i} = \frac{1}{\Delta A} + \frac{1}{\Delta A K_{eq}} \cdot \frac{1}{C_{CD}^i} \quad (S3)$$

The double reciprocal plot of $1/\Delta A_i$ vs. $1/C_{CD}^{i}$ gives a slope of $1/\Delta AK_{eq}$ and an intercept of $1/\Delta A$. The intercept-to-slope ratio can be assumed to be the binding constant $K_{eq}$.

*BH Model from Emission Data*

In the case of a 1:1 stoichiometry, the relation between the fluorescence intensity variation and the CD concentration can be represented as:

$$\frac{1}{\Delta I_i} = \frac{1}{\Delta I_{max}} + \frac{1}{\Delta I_{max} K_{eq}} \cdot \frac{1}{C_{CD}^{i}} \quad (S4)$$

$$K_{eq} = \frac{1}{slope \cdot \Delta I_{max}} \quad (S5)$$

In (4), $\Delta I_i$ and $\Delta I_{max}$ refer to $I_0$ - $I_i$ and $I_{max} - I_0$, in that order, with $I_0$, I, and $I_{max}$ being the emission intensities of TPT in the absence of CD, at an intermediate CD concentration, and at a concentration of complete saturation, respectively, $K_{eq}$ is the binding constant and $C_{CD}^{i}$ is the CD concentration. From the plot of $1/\Delta I_i$ vs. $1/C_{CD}^{i}$, the value of $K_{eq}$ has been determined from the intercept-to-slope ratio.

In both cases, the associated error of $K_{eq}$, $dK_{eq}$, is calculated as:

$$dK_{eq} = \left(\frac{dslope}{|slope|} + \frac{dintercept}{|intercept|}\right) \times |K_{eq}| \quad (S6)$$

**Binding Constant for the Formation of 1:1 and 1:2 Complexes**

In this case, we used the expression:

$$A = \frac{(A_0 + K_1 A_1 [CD] + K_1 K_2 A_2 [CD]^2)}{(1 + K_1 [CD] + K_1 K_2 [CD]^2)} \quad (S7)$$

where A is the absorbance of the system at different concentrations of CD, [CD] is the concentration of DM-βCD in the solution, $A_0$ is the absorbance of RB without DM-βCD, $A_1$ is the absorbance of RB forming 1:1 complex with DM-βCD (this parameter was left free during the fitting process), and $A_2$ is the absorbance of RB forming a 1:2 complex with DM-βCD.

**Application of the Förster Theory for the Non-Radiative Energy Transfer**

Resonant energy transfer is characterized by a rate constant ($k_{DA}$), which expresses the probability of the transfer:

$$k_{DA}(r) = \frac{1}{\tau_D}\left(\frac{R_0}{r}\right)^6 \quad (S8)$$

where $\tau_D$ is the donor fluorescence decay time. $R_0$ is the distance at which the probability of the energy transfer is equal to the probability of the internal deactivation of the excited state of the molecule, and r is the distance between donor and acceptor.

$R_0$ can be expressed as:

$$R_0 = 0.211 \times [\kappa^2 n^{-4} Q_D J(\lambda)]^{(1/6)} \quad (S9)$$

where $\kappa^2$ (the relative orientation in space of the transition dipoles of the donor and the acceptor) is assumed to be 2/3, n (the refractive index) is 1.333, and $Q_D$ (the quantum yield of the donor in the absence of acceptor) is 0.20 (this value corresponds to the quantum yield of the TPT:DM-βCD complex). $J(\lambda)$, the overlap integral, is given by:

$$J = \frac{\int_0^\infty F_D(\lambda)\varepsilon_A(\lambda)\lambda^4 d\lambda}{\int_0^\infty F_D(\lambda)\, d\lambda} \quad (S10)$$

where $F_D(\lambda)$ is the corrected fluorescence intensity of the donor in the wavelength range $\lambda + \Delta\lambda$, with the total intensity normalized to unity, and $\varepsilon_A$ is the extinction coefficient of the acceptor at $\lambda$.

The transfer efficiency can be measured using the relative fluorescence intensity of the donor, in the absence ($F_D$) and presence (FDA) of the acceptor:

$$E = 1 - \frac{F_{DA}}{F_D} \quad (S11)$$

Using the following relationship:

$$E = \frac{R_0^6}{R_0^6 + r^6} \quad (S12)$$

We can calculate r combining Equations S11 and S12. The value of r can be finally used in Equation S8 to estimate the $k_{DA}(r)$ value.